Stagnation of Ablated Metal Vapor in Laser Fusion Reactor with Liquid Wall

Norimatsu[1], T., Furukawa[2], H., Kurahashi[3], S., Shimada[2], Y., Nagatomo[1] H., Kunugi[4],T., Kajimura[5], Y., and Azechi[1], H.

[1] Institute of Laser Engineering, Osaka University, 2-6, Yamada-oka, Suita, Osaka 56500871, Japan
[2] Institute for Laser Technology, 1-8-4 Utsubohonmachi, Nishiku, Osaka 550-0004, Japan
[3] Graduate School of Engineering, Osaka University, 2-1 Yamada-oka, Suita, Osaka 56500871, Japan
[4] Kyoto University, Yoshida-Honmachi, Sakyo-ku, Kyoto 606-8501, Japan
[5] Research Institute for Sustainable Humanosphere, Kyoto University, Uji, Kyoto 611-0011, Japan

E-mail contact of main author: norimats@ile.osaka-u.ac.jp

Abstract. In this paper, formation of clusters by ablated materials and those stagnation at the center of a laser fusion reactor with liquid wall are discussed using improved simulation code DECORE. We will report 1) numerical simulation on formation of clusters immediately before the stagnation 2) preliminary results on the cluster formation at the first bounce of the stagnation, 3) experimental result on the diameter measurement of micro droplets formed in a simulation experiment with back-side irradiation of laser.

1. Introduction

We conceptually designed the laser fusion power plant KOYO-F based on fast ignition scheme and the results were reported at IAEA-FEC 2006[1] and 2008[2]. KOYO-F is a commercial power plant whose electric output is 1 GW. Four modular reactors are powered by 1.2 MJ laser pulses at 4 Hz each from one laser system constructed with cooled Yb:YAG ceramic laser. The size of the chamber room is 3m in the inner radius and 9m in the inner height. The inner surface is covered with a 5-mm thick liquid $Li_{17}Pb_{83}$ flow as the first protective wall[3]. The fusion yield is 200 MJ/shot. Typical heat load by alpha particles is 0.4 MJ/m^2 in 0.05 μs at R=3m. About 8 μm thick LiPb layer is ablated after every shot. In this concept, the chamber clearance after the laser shot is one of our important interests. If ablated LiPb stagnates at the center and lots of clusters are formed, the repetition rate of 4 Hz would be difficult. Although the inner panels are tilted by 30 degree to the tangential direction like a saw teeth to minimize stagnation of ablated materials, some ablated materials will collide at the center and stagnate forming clusters. Since the clusters at the stagnation point will fall by the gravity, it seems difficult to evacuate clusters from the target-firing position before the next target shot.

To discuss the chamber clearance, we have developed an integrated ablation simulation code DECORE (Design Code for Reactor) to clarify the ability of the chamber clearance. The condensation process is based on the B. S. Luk'yanchuk, model[4]. This integrated code can treat wide range of phenomena from microscopic absorption process to macroscopic expansion in the chamber. We estimate the temperatures, the densities, and the velocities of ablated lead instead of LiPb using the simulation code DECORE for the case of first ignition with 200 MJ fusion power. After the ablation, behavior of ablated materials was calculated with ACONPL (Ablation with CONdensation of a Plume).

Another interest in the chamber clearance is formation of liquid droplets caused by hydrodynamic instabilities due to localized heat deposition of alpha particles in the liquid surface. Since the energy spectrum of alpha particles from burning plasma has wide

distribution below 3.6 MeV, the total energy deposition profile along the depth from the liquid metal surface shows its maximum 3 μm below the surface. As the result, the surface is ablated as if a 3 μm thick membrane is peeled off. The membrane is break into small droplets that can not be discussed by above mentioned model. We experimentally simulate the process by irradiating a Pb membrane with a laser pulse from back side and distribution of diameter was measured by using Mie scattering.

2. Stagnation of ablated materials and the influence on target

2.1. Schematic Diagram of simulation code

We numerically simulate ablation, subsequent expansion and stagnation at the center with the simulation code DECORE to discuss the influence on the chamber clearance. DECORE is the 1D Lagrangian code that includes the effects of condensation of a plume, the phase transition from liquid to neutral gas, or partially ionized plasma, the absorption of energies of charged particles, the equation of state, the hydrodynamics, and the radiation transport are included as shown in Fig. 1 (a).

The hydrodynamic process of DECORE consists of energy absorptions of external X-rays and charged particles, phase transitions from liquid to gas to plasma, condensation of a plume, ablation process, hydrodynamics, radiation transport of X-ray. In this paper, this program is named 'ACONPL (Ablation and CONdensation of a PLume)'. Fig. 1(b) is the flow chart of ACONPL. Influence of Li was ignored for simplification. The detail of the simulation code is written elsewhere[5]. We estimate temperatures, densities, and velocities and so on of ablated lead (as a representative of liquid LiPb wall) using DECORE for the case of fast ignition with 200 MJ fusion output.

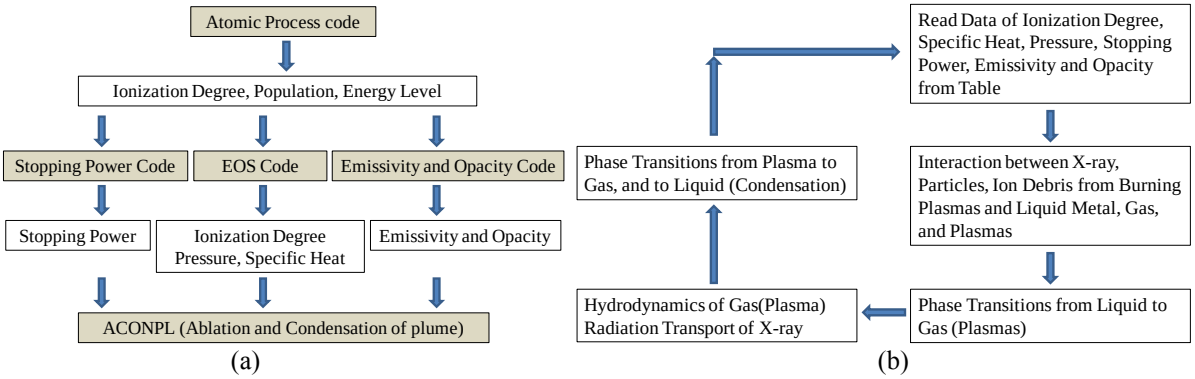

Fig. 1 The schematic diagram of DECORE(a) and the flow chart of ACONPL(b)

In this model, clusters and vapor move together. Therefore, this simulation model is appropriate only before the stagnation at the chamber center. In this parameter range, the mean free path of vapor is larger than the diameter of clusters and the drag forth on the clusters is small. Therefore, clusters move straight into the counter flow after the stagnation.

This simulation code was experimentally checked by observing the diameter of clusters from a planer source that was heated by an electric discharge[6]. The diameter of clusters obtained from the experiment was 30 nm, which was in good agreement with the simulation result.

2.2. Simulation results before the stagnation

Figure 2(a), (b) show space distributions of the number density of all atoms, clusters and the diameter immediately before the stagnation. Here all atoms include those in clusters and surrounding vapor atoms. In these graphs, x=0 m is the chamber wall and x=3 m is the center of the chamber. It is clearly shown that large clusters are formed only near the surface of liquid Pb. In the leading front of the plume no clusters are seen. This can be explained by rapid density decrease due to expansion.

By this time, the temperature and the density on the surface are sufficiently low and the acceleration phase is over. As the result, gasses expand keeping their velocities at this time. If there is no counter plume, clusters with their velocity >24 m/s (or in x>4 mm in another expression) collide with the opposite wall and will be absorbed on the surface that is sufficiently cooled by thermal conduction. Clusters in 0<x<4 mm will expand over the chamber quite uniformly. The amount of atoms in this region is only 1% of ablated lead. The number densities of clusters and all atoms in non-stagnation area of the chamber at the time of the next target injection are estimated to be 1.7 x 10^{7} $cm^{-3}$and 2.7 x10^{14} cm^{-3}, respectively. This number density of Pb atom can be converted to the vapor pressure of 0.13 Torr at 850K which agreed our base line specification for the residual vapor pressure in the chamber of KOYO-F.

When a target is injected into above mentioned chamber and all atoms in the trajectory will adhered on the surface, the thickness of Pb layer on the target surface is calculated to be 100 nm[7, 8]. The high Z layer on the target sometime reduce the target gain because of preheat of the fuel by x-ray emitted from the high Z material on the surface. Our computer simulation on the target gain showed, however, the 100 nm Pb layer on the surface would reduce the target gain from 120 to 100 but it is still acceptable.

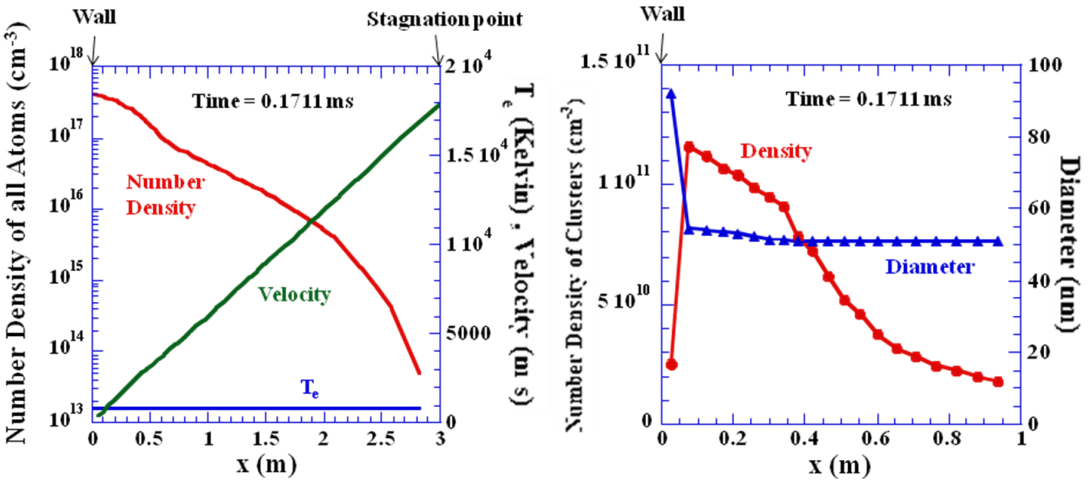

Fig. 2 Distribution of all atoms including those in clusters and vapors before collision at the center (left) and the distribution of clusters at the time (right). The velocity of vapor and clusters (the same in this model) and the diameter of clusters are also shown.

2.3. Simulation after the stagnation

When two counter plumes collide at the center of chamber, atoms from both plumes make a mixing zone. In the early step of the collision, the size of the mixing zone is about 0.5 m that can not be ignored. Originally a Lagrangian-base code can not discuss such mixing zone. We are developing a special code for this zone. In the code, the counter plume is treated as a fluid. Selected particles are injected into the counter plume and the energy transfer and the momentum transfer are calculated until they make the full forward plume. This work is still on the way but preliminary results on the vapor pressure at the stagnation point are shown in Fig. 3. This calculation is a planer model while actual flow in KOYO-F is a cylindrical conversing flow. The peak pressure at the stagnation point exceeded 10^3 Torr. After 1ms, this peak became lower. There were no clusters in the mixing zone because temperature in this zone got higher because of PV work of colliding plumes. When the pressure and temperature decrease, clusters would be formed in the mixing zone.

In future, we had to discuss the influence of non-local clusters that travelled into the mixing zone from surrounding area. In this parameter range, mean free path of atoms is much longer than the diameter of cluster. The kinetic coupling between the cluster and surrounding gas is week. After collision, clusters goes into the mixing zone keeping their velocities almost constant.

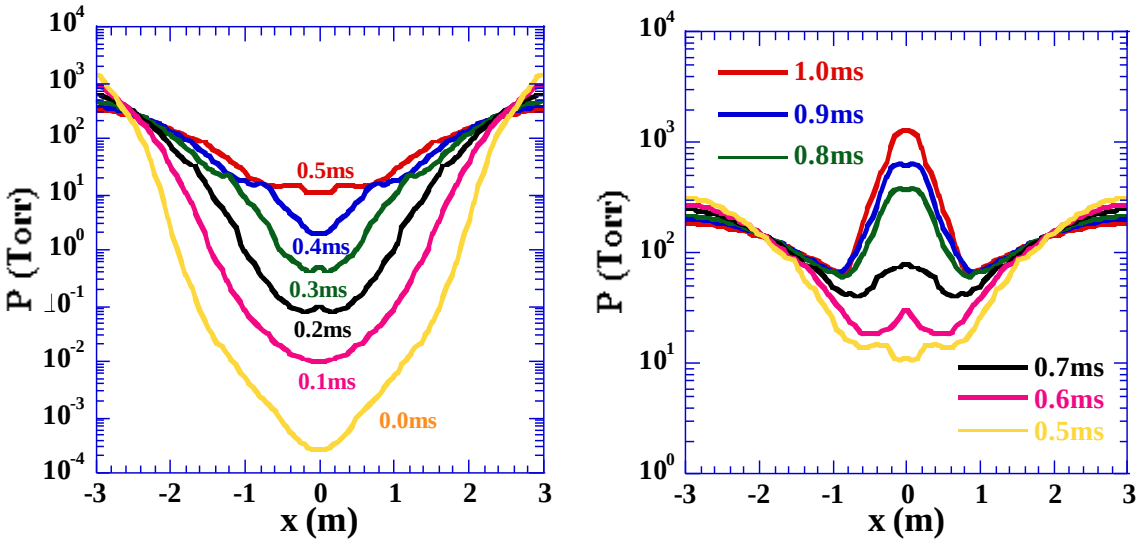

Fig. 3. Pressure profile after the collision. 0<t< 0.5 ms, (a); 0.5<t<1 ms, (b).

3. Liquid particles formed during ablation

3.1. Experiment

When alpha particles bombarded the liquid metal surface, some hydrodynamic instability may happen due to the localized heat deposition along the line perpendicular to the surface. The energy deposited in an area less than 8 μm from the surface but its maximum position is 3 μm below the surface. This deposition profile may cause hydrodynamic instabilities resulting small droplets that can not be discuss by above model. Experimental conditions are summarized in Table I. There are quite large difference between this experiment and those in

KOYO-F. Their hydrodynamic processes in the view point of the instabilities are, however, similar.

Figure 4 shows computer simulation by PINOCO-2D. The upper half of each frame is the density and the lower half is the temperature. Intensity of backlight laser is $2x10^8$ W/cm^2. At 40 ns, the Pb membrane was broken by the RT instabilities and gaseous jets spurted from the surface. We can see many small droplets (dark spots) at t=50 ns.

To experimentally simulate the ablation process by alpha particles, we fired a 4- μm-thick Pb layer on a transparent glass plate from the glass plate side with a 0.08J/pulse, 15 ns, Nd:YAG laser. The laser energy deposits between the Pb membrane and the glass plate, which accelerates the Pb membrane. The glass plate was regarded as a residual LiPb flow. The absorbed laser energy density was estimated to 0.06 MJ/m^2 in 13 ns while the heat load of alpha particles in KOYO-F is 0.4 MJ/m^2 in 50 ns. A plume from the laser spot was back lighted with different timing.

Table I Summary of experimental condition compared with KOYO-F

	Heating process	Heat load (J/cm^2)	Pulse length (ns)	Intensity (GW/cm^2)	Depth of energy absorption peark (μm)
Side wall of KOYO-F (R=3m)	Volume heating	400	50	8	3
Ceiling of KOYO-F (R=9m)	Volume heating	44	150	0.3	3
This experiment	Surface heating	5.2	13	0.4	4

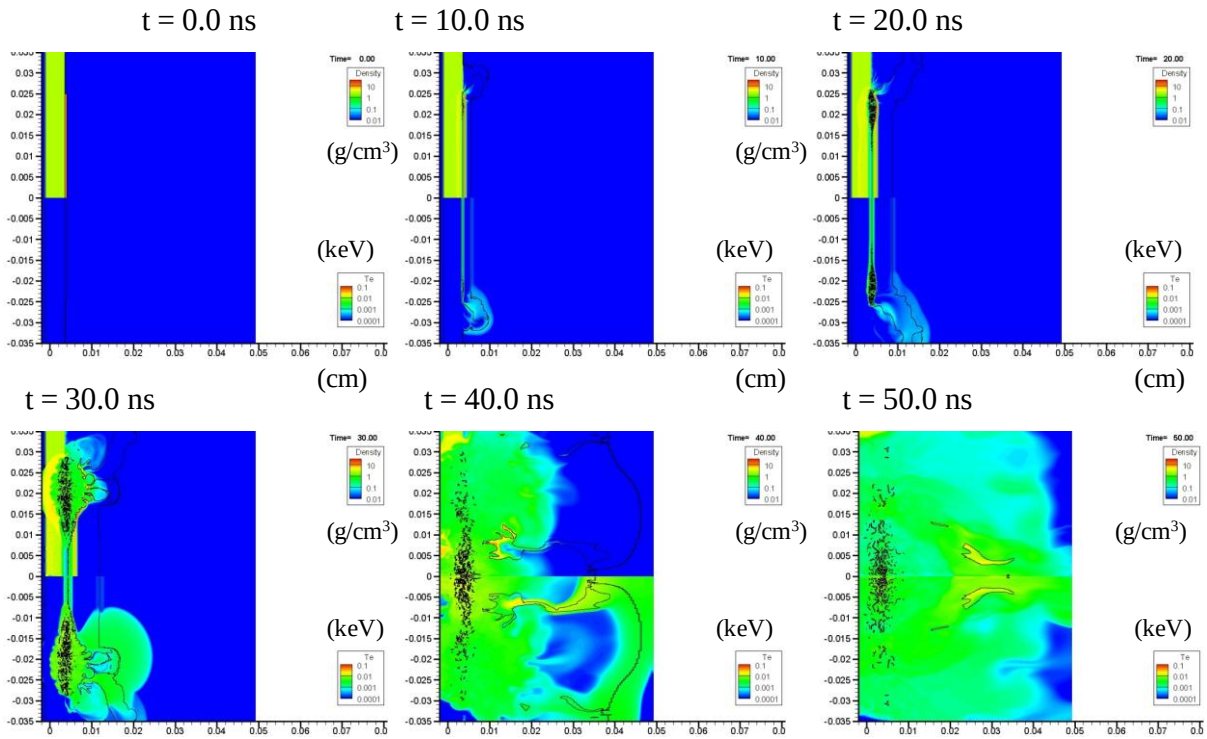

Fig. 4 Computer simulation of back-lighted Pb membrane. Small droplets are formed during the acceleration.

Recently we measured diameter distribution in the ablated plume by Mie scattering method. Figure 5 shows a schematic diagram of experimental setup. In this experiment pure lead was used instead of $Li_{17}Pb_{83}$. A 300 μm diameter, 4 μm thick lead target was prepared on a glass plate by physical vapor deposition. The target was heated to 500 K slightly less than the melting point. This target was irradiated from the glass plate side with a Ne YAG laser whose pulse width, the spot size, the intensity are 13ns, 700-800μm and 4-5×10^{12}W/m^2, respectively. Accelerated (to upward in this figure) plume was illuminated with a 2ω pulse to know the space distribution in flight. The velocity of particles was calculated from images taken at different timings of the probe pulse. The distribution of particle size was measured by Mie scattering. The probe beam was a CW, He-Ne laser whose beam diameter was 5 mm. The detector was a grain spectrometer (NIKKISZO Co. Model 7140-SPR). This instrument gave time and specially integrated diameter distribution in a plume. The diameter resolution was >0.1 μm.

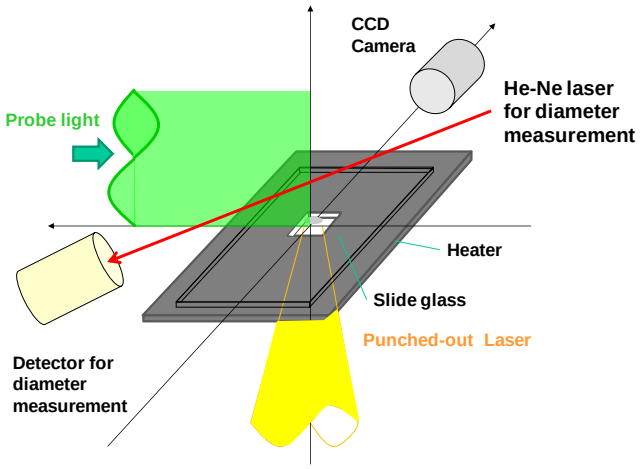

Fig. 5 Illustration to measure particle distribution in the plume.

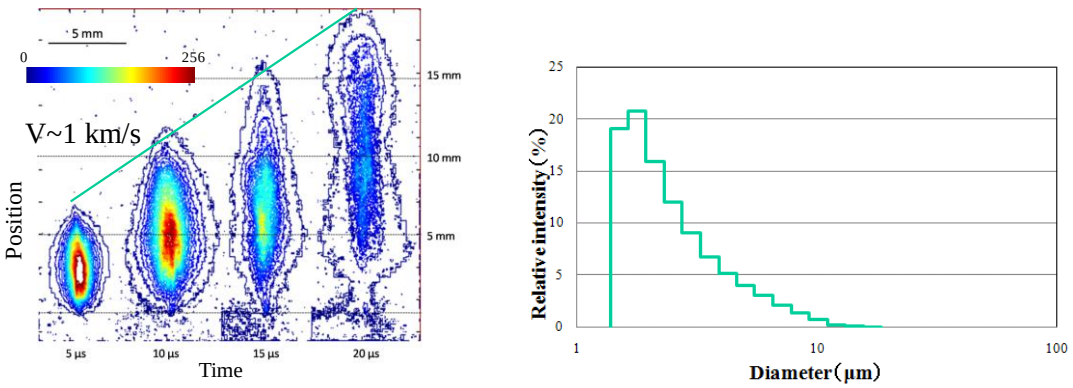

Fig. 6 Distribution of particles in a plume

Measured distribution of particles in a plume is shown in Fig. 6(b). The average diameter was 3.8 μm. This result is quite reasonable when we consider hydrodynamic instabilities. In case of HD instability in ablatively accelerated membrane, middle modes whose special length is close to the thickness breaks the membrane into small pieces first because the growth rate of higher mode saturates soon and, as the result, amplitudes of middle mode exceed those of higher mode.

3.2. Discussions

The velocities of leading front and trailing of the plume were 1000 m/s and 200 m/s, respectively. Since the radius of KOYO-F chamber is 3m and absorbed energy density is larger than this experiment by ten times, we can say these particles will disappear by collisions with the opposite wall before the next target injection. The angular distribution of particles was localized in +/- 10 degree around the perpendicular line to the surface. Since the front panels of the KOYO-F are tilted by 30 degree to the radius direction, these particles leach the opposite wall without stagnation at the center. Ten kg of LiPb will stagnate at the chamber center without this structure. Total mass of stagnated LiPb, however, will be reduced to 0.1 kg with this structure.

Since conditions in this experiment are quite different from alpha heating as shown in Table I, we need more analysis to conclude particle distribution and their behavior in the reactor. For example, formed droplets will be evaporated by low energy alpha particles that reach the surface at a late stage of the alpha heating pulse. Figure 7 shows temporal energy deposition profiles at R=3m where horizontal solid line is the boiling point of lead. In a case of KOYO-F, no particles will be formed at the side wall and the bottom pool. The droplets will be all evaporated by low energy alpha particles. No ablation, however, will happen on the ceiling at R=9m where the areal energy density is 1/10 of that of the side wall. Formation of droplets will take place somewhere between the side wall and the ceiling.

Next necessary discussion is the influence of after glow on the droplets. Here the after glow means hydrogen particle flux that are scattered by alpha particles in the burning plasma. The peak of after glow reach the surface 300 ns after the alpha heat pulse and the intensity is about 1/2 of the alpha heating pulse. Since the Pb vapor leads droplets as shown in Fig. 4, hydrogen atoms will be shield. Actual hydrogen flux on the droplet will be much smaller.

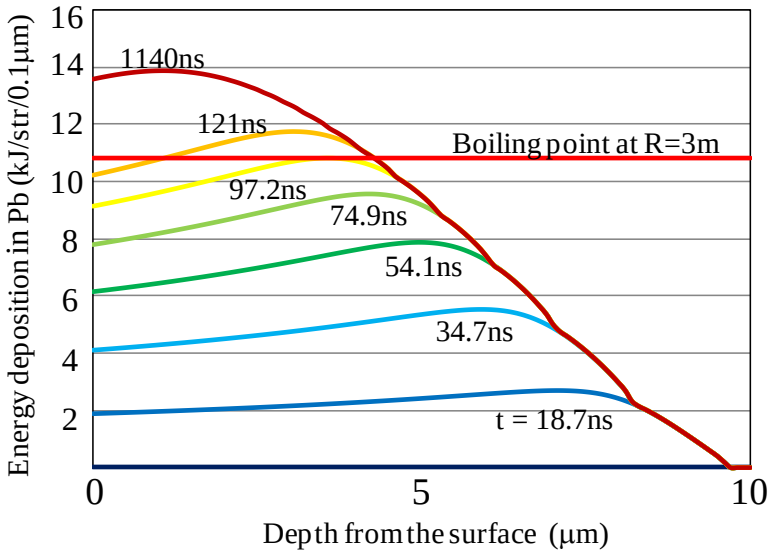

Fig. 7 Temporal profile of energy deposition in liquid 600K Pb. Energy deposition necessary to evaporate Pb at R=3m is also shown.

5. Summary

We have developed an integrated simulation code DECORE that can calculate microscopic energy deposition by alpha particles and subsequent expansion over target chamber in a macroscopic scale considering phase transition between gas and liquid. Clusters are mainly formed near the inner surface but 99% of clusters are absorbed in the opposite liquid wall without the counter plume. Residual 1% clusters remain in the target chamber at the next target injection, but the influence of such clusters is acceptable in the view point of x-ray preheat from the deposited high Z material.

Formation of clusters at the stagnation point is still on the way. Preliminary results indicated that there were no clusters at the stagnation point during $0 < t < 1$ms.

Particles 10 to 100 times larger than clusters would be formed at a limited portion in the reactor by instabilities during the acceleration.

References

[1] T. Norimatsu et al., Presented at IAEA-FEC 2006, Chendo, China. (FT/P5-39)
[2] T. Norimatsu et al., Presented at IAEA-FEC 2008, Geneva, Switzerland (IF/P7-19)
[3] T. Norimatsu, et al., Fusion Science and Technol., **52** (2007) 893-900
[4] B. S. Luk'yanchuk, S. I. Anisimov et. al., SPIE 3618 (1999) 434-452.
[5] H. Furukawa et al., J. Plasma and Fusion Res. Series 8 (2009) 1256-1260.
[6] T. Oshige et. al., J. Phy. :Conf. Series 112 (2008) 032040.
[7] T. Norimatsu, et. al., Fusion Eng. Design. 65 pp393-397 (2003)
[8] T. Norimatsu, et. fl., Fusion Sci. Technol. 43 pp339-345, 2003